

Anisotropy in RFe₂ Intermetallics: An NMR Study

C. Carboni

Department of Physics, College of Science, Sultan Qaboos University, P.O. Box 36, Postal code 123, AlKhod, Muscat, Sultanate of Oman, Email: carlo@squ.edu.om.

NMR : RFe₂

HoFe₂ TbFe₂ TmFe₂ :
mT³⁺ Tb³⁺ oH³⁺.
¹⁶⁵Ho, ¹⁵⁹Tb, ¹⁶⁹Tm
7 2

ABSTRACT: The anisotropy of the Ho³⁺, Tb³⁺ and Tm³⁺ rare-earth ions in RFe₂ compounds is investigated using the field dependence of the NMR spectra of ¹⁶⁹Tm, ¹⁵⁹Tb and ¹⁶⁵Ho in polycrystalline TmFe₂, TbFe₂, HoFe₂ and related pseudo-binary compounds. The very large hyperfine interaction in these ions dominates the NMR spectrum; the NMR frequencies in the 2 to 7 GHz range provide therefore a measure of the localized $4f$ moment and its orientation in the crystal field. We compare the NMR measurements to single ion computations that include magnetostriction.

KEYWORDS: Cubic laves phases, Rare-earth intermetallic, Hyperfine splitting, Magnetic anisotropy, NMR.

1. Introduction

The cubic Laves phases series RFe₂ where R is a rare-earth element is the simplest of the several intermetallic compounds in which rare-earth and iron magnetism coexist. For more than 30 years the RFe₂ compounds and their pseudo-binary (RR') Fe₂ and R(FeM)₂ alloys where M is a transition metal have been the subject of intense investigations. These compounds have provided and continue to provide (Sawickki *et al*, 2000) a fertile ground to test theoretical models. More recently epitaxially grown films (Lee *et al*, 2000, de la Fuente *et al*, 2001, Gordeev *et al*, 2001, Oster *et al*, 2005), X-ray magnetic circular dichroism investigations (Fujiwara *et al*, 2005, Dumesnil *et al*, 2002, Parlebas *et al*, 2006) and the hydrated RFe₂ materials (Paul-Boncour, 2004) have attracted the attention of several researchers. However, there are some basic questions in the RFe₂ that are not yet completely resolved. There is still uncertainty about the anisotropy of the iron sub-lattice, about the

contribution of magneto-elastic effects to the measured anisotropy (Mougin *et al*, 2000), about the crystal-field interaction at the lanthanide site and about the role of the ordered super-lattice of vacancies in the C15 Laves phases (Gratz *et al*, 1996). Also, the distribution of the total magnetization between the iron and lanthanide sub-lattices and the relative contribution of localized and itinerant moments is still an open question (Fujiwara *et al* 2005).

In the present paper the anisotropy of the rare-earth ion is investigated using the field dependence of the NMR spectra of ^{169}Tm ($I = 1/2$), ^{159}Tb ($I = 3/2$) and ^{165}Ho ($I = 7/2$) in polycrystalline TmFe_2 , TbFe_2 , HoFe_2 and some pseudo-binary compounds. In the Ho^{3+} , Tb^{3+} and Tm^{3+} ions the very large hyperfine interaction dominates the NMR spectrum; the NMR frequencies in the 2 to 7 GHz range provide therefore a measure of the localized $4f$ moment and its orientation in the crystal field. We compare our NMR measurements to single-ion computations that include the distortion of the cubic environment of the lanthanide ion due to the magnetostriction. The results from the computation suggest that the magnetostriction does not have a significant effect on the NMR spectrum.

2. Theory

In this section we describe the model used for the computation of the magnitude and the orientation of the moments in RFe_2 compounds subjected to a magnetic field applied in any arbitrary direction but before doing so, we need to clarify a possible confusion between two senses of the term ‘‘anisotropy’’.

There are two distinct aspects to the anisotropy of a magnetic material, the *energy anisotropy* and the *magnetization anisotropy*. The former, conventionally specified by classical ‘‘anisotropy constants’’ denotes the angular variation of the free energy, whereas the latter denotes the angular variation of the magnitude of the ionic moment. For the RFe_2 compounds in which the exchange interaction \mathbf{H}_{ex} may, at least to a first approximation, be considered isotropic both types of anisotropy are manifestations of the crystal-field interaction \mathbf{H}_{cf} at the lanthanide site. The relationship between energy and magnetization anisotropy is not straightforward. For example, it is not necessarily the case that the hardest direction of magnetization (i.e. the direction for which the free energy is greatest) is the direction in which the ionic moment is most quenched. The crystal-field interaction \mathbf{H}_{cf} in the RFe_2 is a small perturbation on the exchange interaction \mathbf{H}_{ex} the energy anisotropy may thus be regarded as a quasi-classical effect of first order in \mathbf{H}_{cf} . The magnetization anisotropy, on the other hand, is an essentially quantum mechanical effect associated with those terms in \mathbf{H}_{cf} that do not commute with \mathbf{H}_{ex} . The quenching of the ionic moment is a second order effect varying as the ratio of square of the strength of \mathbf{H}_{cf} to that of \mathbf{H}_{ex} . A fuller discussion of these points can be found in section 4.4 of McCausland and Makenzie (1979).

2.1 The effective electronic Hamiltonian

The orientation of the lanthanide and the iron moments in a crystal of RFe_2 subjected to a magnetic field applied at an arbitrary angle is a compromise between several competing interactions. There is the ferrimagnetic coupling between the lanthanide and the iron, the crystal-field interaction, the interaction with the applied field and indirectly the magnetostriction which affects the crystal field. If one assumes that the iron sub-lattice is isotropic in both senses, the magnitude of the iron moment is constant and its direction always collinear to the total field $\mathbf{B}_{\text{tot}}^{\text{Fe}}$ at the iron site, the equilibrium orientation of the two moments in the presence of a field applied at an arbitrary direction is as shown on Figure 1. The total field at the lanthanide site is $\mathbf{B}_{\text{tot}}^{\text{Ln}} = \mathbf{B}_a - \lambda \mathbf{m}$ where \mathbf{m} is the iron moment and λ the lanthanide-iron exchange constant.

The lanthanide ion is described by the effective electronic Hamiltonian

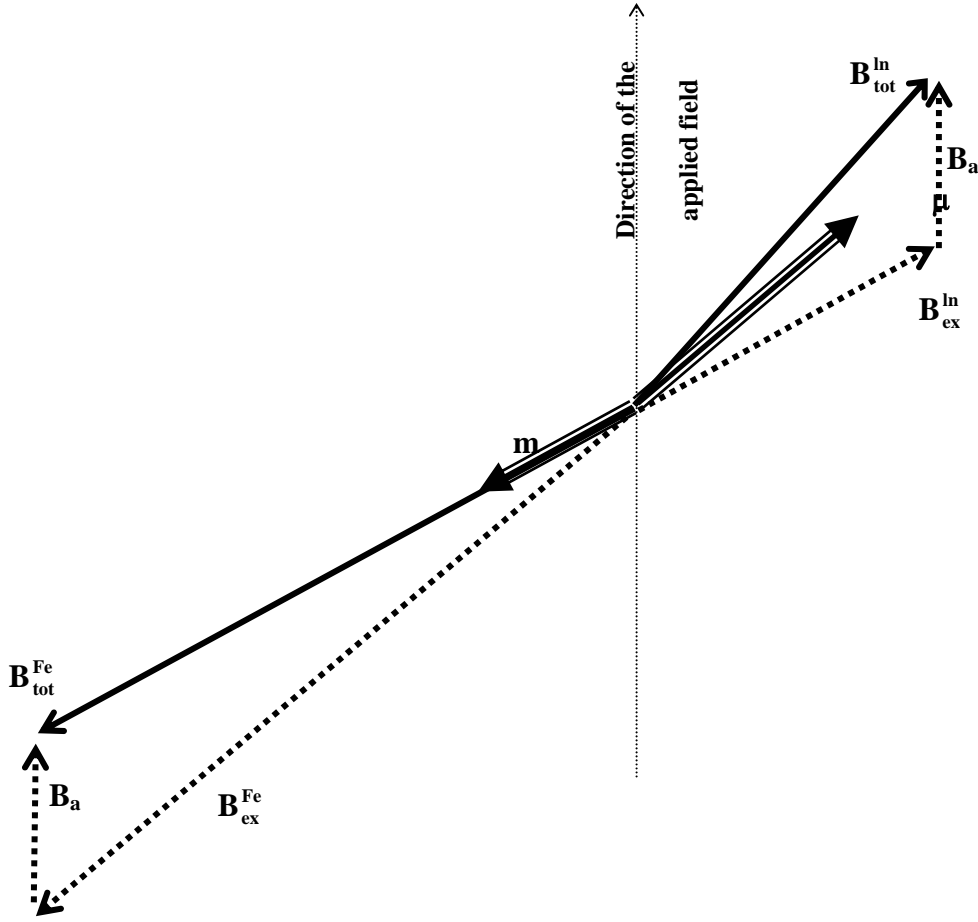


Figure 1. The orientation with respect to the direction of the applied field B_a of the iron moment m , the lanthanide moment μ , the total field B_{tot}^{ln} at the lanthanide site and the total field B_{tot}^{Fe} at the iron site. B_{ex}^{Fe} and B_{ex}^{ln} are respectively the exchange field seen by the iron and the exchange field seen by the lanthanide ion.

$$H_{el} = B_4 O_4 + B_6 O_6 + V_2 - B_{tot}^{ln} \cdot \mu \quad (1)$$

where the $B_n O_n$ denote the cubic crystal-field terms in the notation of Lea, Leask and Wolf (1962). The operators O_4 and O_6 are respectively combinations of fourth order and sixth order Stevens operators equivalent (Stevens 1952); the explicit form of these operators is given in the appendix. The term V_2 is the second order crystal-field term arising from the distortion of the cubic environment of the ion caused by magnetostriction (Buschow 1977).

$$V_2 = \frac{2K_{me}}{J(2J-1)} [k_1 k_2 (\mathbf{J}_1 \mathbf{J}_2 + \mathbf{J}_2 \mathbf{J}_1) + k_2 k_3 (\mathbf{J}_2 \mathbf{J}_3 + \mathbf{J}_3 \mathbf{J}_2) + k_3 k_1 (\mathbf{J}_3 \mathbf{J}_1 + \mathbf{J}_1 \mathbf{J}_3)] \quad (2)$$

where \mathbf{K} is a unit vector parallel to the total angular momentum \mathbf{J} of the $4f$ electrons of the ion and K_{me} is the magneto elastic constant. The indices 1, 2 and 3 denote respectively the directions of the three four-fold axis of the cubic unit cell.

The crystal-field parameters are phenomenological parameters determined experimentally. In transparent compounds these parameters can be accurately obtained from the optical absorption spectrum. In metals the determination of the crystal field parameters is not straightforward; they are obtained by combinations of different experimental techniques which can produce conflicting results (McMorrow *et al*, 1989). For the RFe₂ series there is to our knowledge no detailed comprehensive analysis for the crystal field parameters. To date the most widely accepted sets of crystal field parameters for the RFe₂ are the ones obtained by Germano and Butera (1981). The parameters for the Tb, Ho and Tm compounds are given in Table 1 together with the exchange and the magnetoelastic constant. Germano and Butera obtained the crystal field parameters from specific heat measurements. In their analysis the magnetostriction is not taken into account, the site symmetry is considered exactly cubic; this plus the fact that the contribution from the crystal field to the specific heat is relatively small may raise questions concerning the accuracy of the parameters. Nevertheless most of the predictions based on these parameters are in fairly good agreement with experiments; these parameters are used *faute de mieux* for the present work. The computed direction of spontaneous magnetization in HoFe₂, TmFe₂ and TbFe₂ at zero temperatures is respectively the $\langle 100 \rangle$, $\langle 110 \rangle$ and $\langle 111 \rangle$ direction.

Table 1. The exchange fields, the crystal-field parameters and the magnetoelastic constants obtained by Germano and Butera (1981) for HoFe₂, TbFe₂ and TmFe₂.

	λ_m (T)	$10^4 B_4$ (K)	$10^6 B_6$ (K)	K_{me} (K/ion)
TbFe ₂	162	101	20	-13
HoFe ₂	108	-9.26	5.1	-1.7
TmFe ₂	70	55	35	-9.0

In TmFe₂ the computation reveals a low-lying first excited state that strongly prefers the $\langle 111 \rangle$ direction. The existence of this excited state is responsible for the reorientation of the magnetization at about 55 K reported by Germano and Butera. Above 55 K the $\langle 111 \rangle$ direction is the preferred orientation for the magnetization. The experiments reported in the present work were carried out at liquid-helium temperatures where only the ground state is significantly populated therefore the $\langle 110 \rangle$ direction is strongly preferred in TmFe₂.

2.2 Computation

In zero applied field and in the absence of magnetostriction the ground state and ground state energy of the lanthanide ion can be readily obtained from the Hamiltonian 1. The expectation value of $\langle \mathbf{J}_z \rangle$ for the ground state is then obtained to calculate the intra-ionic contribution to the hyperfine splitting and the rare-earth's moment. In the presence of an applied field at an arbitrary orientation one must first determine the orientation of B_{tot}^{ln} .

To determine the equilibrium orientation of B_{tot}^{ln} in an applied field we have minimized with respect to the polar angles of the iron moment, θ_{Fe} and ϕ_{Fe} the free energy per formula unit at absolute zero including the magnetostriction. At zero temperature the free energy is simply

ANISOTROPY IN RFe₂ INTERMETALLICS

$$F = U - TS = U = \langle H_{el} \rangle + \langle H_{Fe} \rangle, \quad (3)$$

where $\langle H_{Fe} \rangle = 2(\mathbf{B}_a - \lambda \langle \boldsymbol{\mu} \rangle) \cdot \mathbf{m}$ is the contribution from the iron sub-lattice and the expectation values are calculated using the ground state of the lanthanide ion. In writing equation (3) it is implicitly assumed that the iron sub-lattice is isotropic in both senses.

The minimization of the free energy (3) is not straightforward. The term V_2 depends on the orientation of the lanthanide moment that is itself the object of the computation. The computation was done by iterations. An educated guess of the orientation of the lanthanide moment was used for the first iteration. The computation was repeated until self-consistency and minimum energy was achieved. It was observed that the term V_2 does not affect significantly the outcome of the computation.

In order to investigate the behavior of polycrystalline samples in applied fields we have computed the magnitude and orientation of the lanthanide moment in HoFe₂, TbFe₂ and TmFe₂ at various fields applied in 30 different orientations equally spaced over the portion of the unit sphere defined by the <100>, <110> and <111> directions. The results for the 8 T field are summarized in Table 2 and Figure 2. Figure 2 is a planar projection of the portion of the unit sphere under consideration. The orientation of the moment is represented on the Figure by a point corresponding to the intersection of the direction of the moment and the surface of the unit sphere. The shaded areas around the <100>, <110> and <111> axis represent the loci of the direction of the holmium, the thulium and the terbium moments respectively, when the direction of the applied field is scanned across the entire area of the unit sphere under consideration. One can see that an 8 T field applied in any direction hardly moves the thulium moment away from its <110> preferred orientation, 5 degrees at most when the field is along the <111> direction. Holmium, on the other hand, can be more readily moved away from the <100> preferred orientation, 25 degrees when the field is along the <110> axis.

Table 2. The computed orientation of the iron's magnetic moment \mathbf{m} , the lanthanide magnetic moment $\boldsymbol{\mu}$ and the total field \mathbf{B}_{tot}^{ln} at the lanthanide site for an 8 tesla field applied along each of the principal crystallographic directions. The column before last gives the computed intra-ionic contribution to the dipolar hyperfine splitting and the last column gives the total field-dependent contribution (intra-ionic plus the contribution from applied field). ψ is the angle between the applied field and the lanthanide moment.

Ion	\mathbf{B}_a		\mathbf{m}		\mathbf{B}_{tot}^{ln}		$\boldsymbol{\mu}$		$a' = a\langle J \rangle_z$ (MHz)	$a' + \gamma B \cos \psi$ (MHz)
	θ	ϕ	θ	ϕ	θ	ϕ	θ	ϕ		
Tb ³⁺	0	0	54.0	45	52	45	52	45	3171	3219
	45	0	54.2	44	53	43	54	43	3171	3236
	54.7	45	54.7	45	54.7	45	54.7	45	3171	3250
Ho ³⁺	0	0	0	0	0	0	0	0	6488	6559
	45	0	25	0	27	0	26	0	6479	6546
	54.7	45	13	45	15	45	13.5	45	6484	6537
Tm ³⁺	0	0	48	0	44	0	44	0	2308	2328
	45	0	45	0	45	0	45	0	2309	2337
	54.7	45	45	0	45	5	45	4	2308	2331

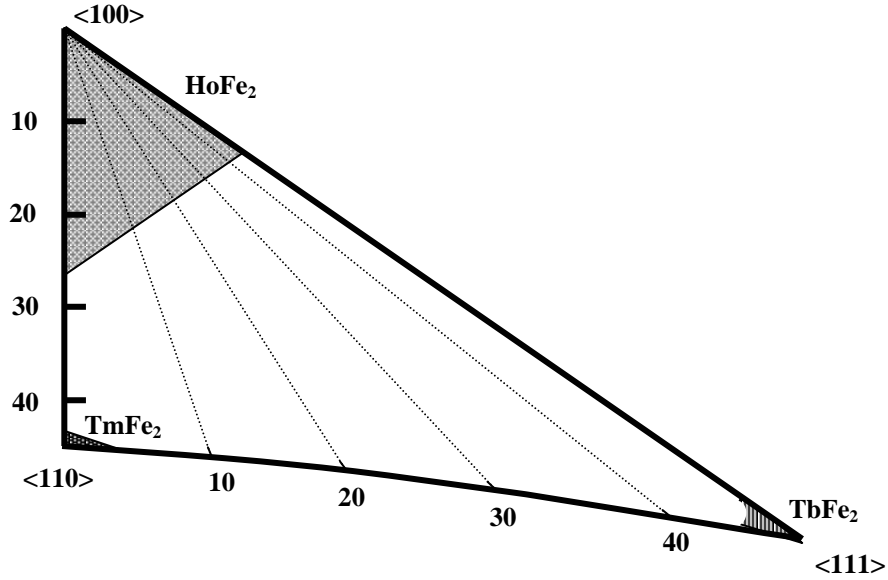


Figure 2. The planar projection of the portion of the unit sphere under consideration. The angles along both axes are in degrees. The shaded areas around the $\langle 100 \rangle$, $\langle 110 \rangle$ and $\langle 111 \rangle$ axis represent the loci of the direction of the holmium, the thulium and the terbium moments respectively, when the direction of an applied 8 T field is scanned across the entire area of the unit sphere under consideration.

Table 2 gives the computed polar angles of the iron moment \mathbf{m} , the lanthanide moment $\boldsymbol{\mu}$ and the total field at the lanthanide site $\mathbf{B}_{\text{tot}}^{\text{ln}}$ when the 8 tesla field \mathbf{B}_a is applied along each of the principal crystallographic orientations. The last two columns give computed field dependent contributions to the dipolar hyperfine splitting which will be discussed in the next section.

2.3 The hyperfine splitting

The theory of the hyperfine splitting in rare-earth compounds is described in detail in McCausland and Makenzie (1979), Bunbury *et al* (1989) and Li *et al* (1996) whose notation we shall follow. The hyperfine splitting of the electronic states is described to first order by the effective nuclear spin Hamiltonian

$$\mathbf{H} = h \left\{ a_t \mathbf{I}_z + P_t \left(\mathbf{I}_z^2 - \frac{1}{3} \mathbf{I}^2 \right) \right\} \quad (4)$$

where \mathbf{I} is the nuclear spin, a_t and P_t are respectively the dipolar and the quadrupolar hyperfine parameters.

The z-axis is chosen to be parallel to $\langle \mathbf{J} \rangle$. Preliminary computations have shown that in the exchange dominated RFe_2 compounds second order contributions to the hyperfine parameters are at most 0.05%. Therefore, the second order terms (Bunbury *et al* 1989) have been neglected in the present work. Because of the strong hyperfine coupling in Ho^{3+} , Tb^{3+} and Tm^{3+} the total dipolar hyperfine constant is dominated by the dipolar intra-ionic term

$$a' = a \langle J_z \rangle \quad (5)$$

where a , the dipolar hyperfine coupling constant, is 6497 MHz for Ho³⁺, 3180 MHz for Tb³⁺ and 2333 MHz for Tm³⁺, the intra-ionic contribution a' is therefore very sensitive to small variations of the $4f$ moment and provides an accurate measure of the moment.

The extra-ionic contribution to the dipolar splitting is

$$a'' = \left(\frac{g_n \mu_n}{h} \right) \mathbf{B}_z'' \quad (6)$$

where \mathbf{B}_z'' is the component along \mathbf{J} of \mathbf{B}'' the extra-ionic field at the lanthanide nucleus. \mathbf{B}'' is the vector sum of various terms

$$\mathbf{B}'' = \mathbf{B}_a + \mathbf{B}_{\text{dip}} + \mathbf{B}_p + \mathbf{B}_n \quad (7)$$

where \mathbf{B}_a is the applied field, \mathbf{B}_{dip} is the dipolar field, \mathbf{B}_p is the field due to conduction electrons polarized by the spin of the parent ion and \mathbf{B}_n is the transferred hyperfine field from neighboring rare-earth and iron ions.

To a good approximation ($\mathbf{B}_{\text{dip}} + \mathbf{B}_p + \mathbf{B}_n$) can be regarded as independent of the applied field. Since we are interested in the field dependence of the hyperfine splitting, we will consider the field independent part of the extra-ionic contribution to the dipolar hyperfine splitting

$$a_{\text{thf}} = (g_n \mu_n / h) (\mathbf{B}_{\text{dip}} + \mathbf{B}_p + \mathbf{B}_n) \quad (8)$$

as a free parameter to be determined from the zero-field NMR spectrum; a_{thf} is equal to the difference between the computed intraionic contribution and the measured total dipolar hyperfine parameter in zero fields. The total dipolar hyperfine splitting is therefore

$$a_t = a_{\text{thf}} + a' + \gamma \mathbf{B} \cos \psi \quad (9)$$

where ψ is the angle between the applied field and the lanthanide moment and γ is the gyromagnetic factor.

The field dependent contribution ($a' + \gamma \mathbf{B} \cos \psi$) computed in a field of 8 T applied along each of the three principal crystallographic axis is given in Table 2.

3. Experiment.

The compounds were prepared by melting the constituents in an arc furnace under an atmosphere of purified argon. For the thulium compounds, the starting materials contained a 3% excess of Tm to compensate for the anticipated loss by evaporation. The resulting ingots were re-melted three times, annealed for two weeks at 900 °C and finally crushed to form a fine powder sample. X-ray examination revealed less than 5% of non-Laves phases. Approximately 5 mg of the powder, embedded in epoxy resin, was located close to the current antinode of the central conductor of a tunable coaxial resonator of the type described by McCausland and Makenzie (1979). The NMR measurements were carried out at 1.3 K and 4.2 K in magnetic fields up to 8 T using the microwave spin-echo spectrometer described by Carboni *et al* (1989). The spectra were obtained by varying the frequency at fixed values of the applied field.

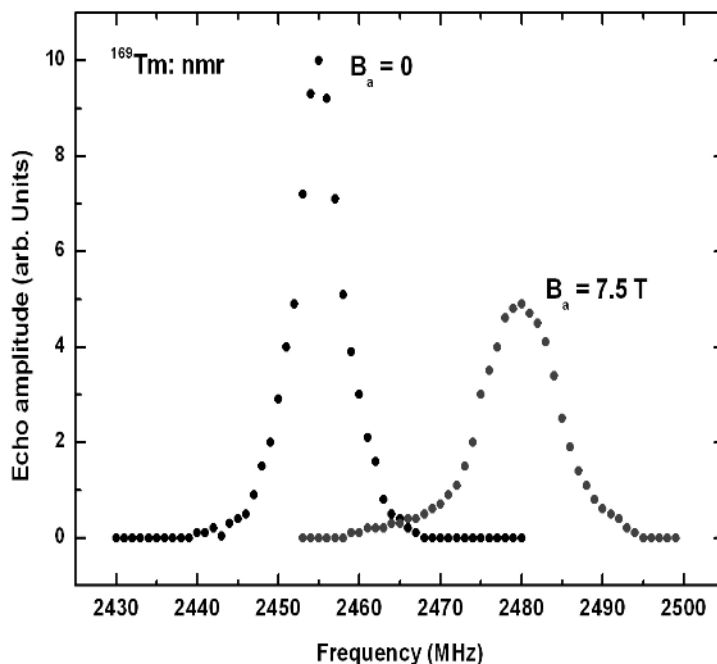


Figure 3. The ^{169}Tm NMR line of thulium in TmFe_2 in zero fields and in an applied field of 7.5 T.

For TmFe_2 and TbFe_2 the measured relaxation times are of the order of several micro seconds which is an order of magnitude larger than the pulse separation (200 ns) used to take the spectra so the NMR lines are negligibly distorted by relaxation. In pure HoFe_2 the transverse relaxation time is of the order of 200 ns, too short to obtain a reliable spectrum. The seven lines of the ^{165}Ho ($I = 7/2$) spectrum could not be unequivocally identified. The ^{165}Ho NMR data presented here were obtained mainly from specimens with a few percent of holmium substituted in TmFe_2 , LuFe_2 and YFe_2 where the relaxation times are less prohibitive and the spectra in low fields are resolved. The spectrum of ^{159}Tb ($I = 3/2$) consists of three lines; because of the strong quadrupolar hyperfine coupling the lines are very well resolved; the separation between the lines is of the order of 350 MHz. The spectrum of ^{169}Tm ($I = 1/2$) consists of a single line.

A summary of the hyperfine parameters measured in the various compounds investigated at liquid helium temperatures and in zero fields is given in Table 3. For comparison previously published data from other R': RFe_2 materials have also been included in the table.

4. Discussion.

The NMR line of $^{169}\text{Tm}:\text{TmFe}_2$, in zero fields and in an applied field of 7.5 tesla are shown in Figure 3. The field dependence of the measured total hyperfine parameter a_t of $^{169}\text{Tm}:\text{TmFe}_2$, is shown in Figure 4-a; the variation is linear with a slope of (3.42 ± 0.05) MHz/T.

The slope is less than the value of 3.52 MHz/T expected for the nuclear spin parallel to the applied field. We also observe that the applied field causes only a small broadening of the NMR line (see Figure 5).

ANISOTROPY IN RFe₂ INTERMETALLICS

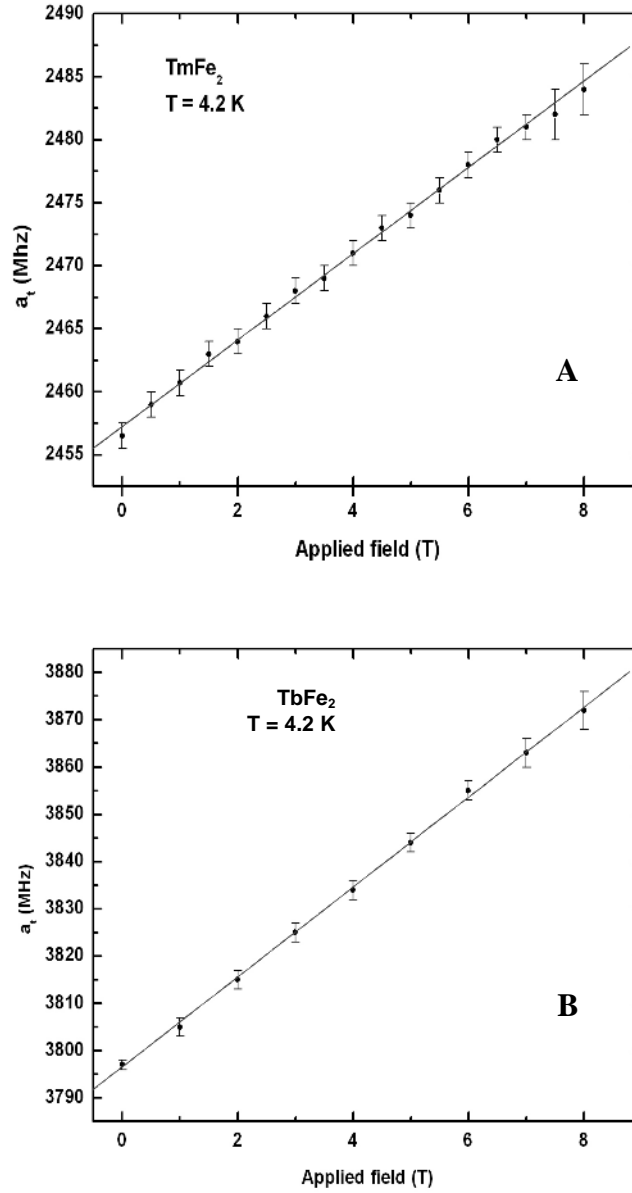


Figure 4. The measured total dipolar hyperfine parameter of ¹⁶⁹Tm:TmFe₂ and ¹⁵⁹Tb:TbFe₂ as a function of the applied field.

These two observations confirm the prediction from our computations that the moment of the Tm³⁺ ion in all the crystallites of the specimen has remained close to the <110> orientation even at high fields. The computation

C. CARBONI

shows that there is a significant quenching of $\langle J_z \rangle$ if the moment is rotated away from the $\langle 110 \rangle$ orientation with a concomitant reduction of the hyperfine splitting. The reduction is 28% if the thulium moment is forced along the $\langle 100 \rangle$ direction corresponding to a shift of more than 350 MHz in the NMR frequency. Therefore, if the rare-earth moments rotate to become close to the direction of the applied field one expects a line broadening of the order of 200 to 300 MHz. This is not observed.

When the thulium ion is placed in a non magnetic and isotropic host like 1% ^{169}Tm (Tm:LuFe₂) we observe that a_t decreases with applied field with a slope of (-13 ± 2) MHz/T, much larger than the -3.52 MHz/T expected for the nuclear spin anti-parallel to the applied field. The line broadens rapidly with the applied field; the line width is 10 MHz in a field of 0.7 T and the line is too broad for reliable measurements in a field of 1 T. Assuming that the lutetium sub-lattice does not contribute significantly to the anisotropy these observations can be interpreted as follows: the applied fields causes a significant rotation of the iron moments towards a direction parallel to the applied field. Because of the strong ferimagnetic coupling between the thulium ion and the iron sublattice, the thulium moments are gradually rotated away from the strongly preferred $\langle 110 \rangle$ orientation hence the sharp reduction in the intraionic contribution to a_t and the line broadening. Finally we note from table 3 that when the thulium ion is placed in the HoFe₂ host there is an *increase* of about 10 MHz in the dipolar hyperfine parameter and not the expected *reduction* of about 350 MHz if the thulium moment was forced along the $\langle 100 \rangle$ orientation preferred by the HoFe₂ host. One can conclude that thulium moment has remained close to the $\langle 110 \rangle$ direction and that therefore the iron together with the holmium sublattice are not along the $\langle 100 \rangle$ direction. The increase in the dipolar hyperfine parameter is due to the larger transferred hyperfine field in the holmium host due the fact that Ho³⁺ has a larger projected spin ($\sigma_{\text{Ho}} = 2.0$) than Tm³⁺ ($\sigma_{\text{Tm}} = 1.0$) (McCausland and Makenzie, 1979). A refined analysis of the data presented in this section is still in progress and will be presented in a separate publication (Carboni *et al* 2009, to be published).

Table 3. The measured hyperfine parameters of Tm³⁺, Ho³⁺ and Ho³⁺ in various RFe₂ hosts. (a) Li *et al* (1996), (b) De Azevedo (1986). (c) Al Assadi *et al* (1984).

Nucleus and host	a_t (MHz)	P_t (MHz)
$^{169}\text{Tm}:\text{TmFe}_2$	2456 ± 2	-
1% ^{169}Tm (Tm:Ho Fe ₂)	2467 ± 2	-
1% ^{169}Tm (Tm:Lu Fe ₂)	2445 ± 2	-
^{169}Tm (Tm:Y Fe ₂) (a)	2422 ± 2	-
^{169}Tm (Tm:Gd Fe ₂) (a)	2466 ± 2	-
1% ^{165}Ho (Ho:TmFe ₂)	6920 ± 5	60 ± 1
3% ^{165}Ho (Ho:LuFe ₂)	6850 ± 10	57 ± 2
^{165}Ho (Ho:YFe ₂) (c)	6860 ± 10	59 ± 2
^{165}Ho (Ho:GdFe ₂) (c)	6986 ± 10	
$^{159}\text{Tb}:\text{TbFe}_2$	3798 ± 3	345 ± 2
^{159}Tb (Tb:LuFe ₂) (b)	3693 ± 3	349 ± 2
^{159}Tb (Tb:GdFe ₂) (b)	3822 ± 3	356 ± 2

The field dependence of the measured total dipolar hyperfine parameter a_t of $^{159}\text{Tb}:\text{TbFe}_2$, is shown on Figure 4-b; the variation is linear with a slope of (9.5 ± 0.1) MHz/T. The field dependence of the line-width is given in Figure 5. The data shows that like for TmFe₂ the anisotropy is, as predicted by the computation, very large and the terbium ion remains close to the $\langle 111 \rangle$ direction even at high fields. A detailed investigation of the zero field hyperfine splitting of Tb³⁺ in various RFe₂ hosts has been done by W M de Azevedo (de Azevedo, 1986 and de Azevedo *et al* 1985).

Except in the TmFe₂ host, the NMR spectra from ^{165}Ho in the RFe₂ hosts are poorly resolved because the transverse relaxation time is comparable to the minimum pulse separation available on the spectrometer.

Moreover, the NMR lines broaden rapidly with the applied field hence the large uncertainty on the hyperfine parameters for the holmium given in table 3. In the HoFe₂ compound it was not possible to obtain the complete 7-lines spectrum therefore it was not possible to obtain a value for the dipolar hyperfine parameter. The quadrupolar parameter P_1 obtained from the spacing between adjacent lines for this compound is (55 ± 5) MHz.

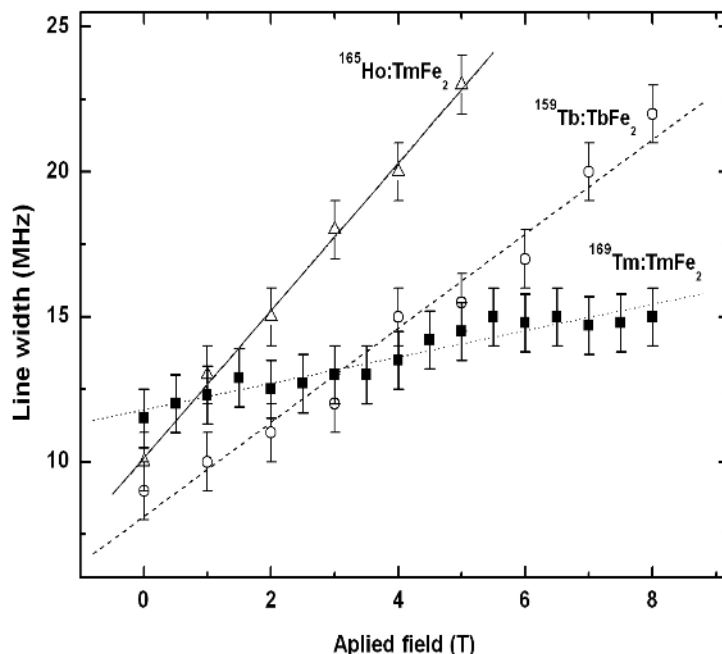


Figure 5. The behavior of the line width of the central line of the NMR spectra of ¹⁶⁹Tm:TmFe₂, ¹⁵⁹Tb:TbFe₂ and ¹⁶⁵Ho: Ho(TmFe₂).

For holmium in the TmFe₂ host the spectrum is well resolved in fields up to 5 T. However, as can be seen in Figure 5, the line-width increases sharply with the applied field. If one assumes that the line broadening is mainly due to a spread of the orientations of the Ho³⁺ moments with respect to the crystallites axis then, since it has been established that the Tm³⁺ moment remains along the <110> direction, one can conclude that the applied field does, as predicted by the computation, achieve some rotation of holmium moment away from the <100> direction. The slope of a_1 versus field is (8.3 ± 0.2) MHz/T, significantly less than the expected 8.9 MHz/T; this is almost certainly due to a gradual quenching of the holmium moment as it is rotated away from its preferred direction.

5. Acknowledgements

The experimental part of this work was done during the time the author was at the University of Manchester (UK) supported by grants from the UK Engineering and Physical Science Research council (EPSRC). The author is also grateful to Prof MAH McCausland and Dr D StP Bunbury for comments, discussions and support.

Appendix

The Steven operator equivalent pertaining to a site of cubic symmetry.

$$O_4^0 = 35J_z^4 - [30J(J+1) - 25]J_z^2 - 6J(J+1) + 3J^2(J+1)^2$$

$$O_4^4 = \frac{1}{2}(J_+^4 + J_-^4)$$

$$O_6^0 = 231J_z^6 - 105[3J(J+1) - 7]J_z^4 + [105J_z^2(J+1)^2 - 525J(J+1) + 294]J_z^2$$

$$- 5J^2(J+1) + 40J^2(J+1)^2 - 60(J(J+1))$$

$$O_6^4 = \frac{1}{4}[11J_z^2 - J(J+1) - 38](J_+^4 + J_-^4) + \frac{1}{4}(J_+^4 + J_-^4)[11J_z^4 - J(J+1) - 38]$$

In the notation of Lea Leak and Wolf:

$$\mathbf{O}_4 = \mathbf{O}_4^0 + 5\mathbf{O}_4^4$$

$$\mathbf{O}_6 = \mathbf{O}_6^0 - 21\mathbf{O}_6^4$$

6. References

- AL ASSADI, K.F., MACKENZIE, I.S. and McCAUSLAND, M.A.H. 1984. Domain and domain-wall nuclear magnetic resonance of ^{265}Ho in $(\text{Gd,Y})\text{Fe}_2$, *J Phys F: Met. Phys* **14**: 525.
- BUNBURY, D.ST.P., CARBONI, C. and McCAUSLAND, M.A.H. 1989. Field dependence of the hyperfine splittings in holmium hydroxide *J. Phys. Condens. Mat.* **1**: 1307.
- BUSHOW, K.H.J. 1977. Intermetallic compounds of Rare Earth and 3-d transition metals, *Rep Prog Phys* **40**: 1179-1256.
- CARBONI, C., MACKENZIE, I.S. and McCAUSLAND, M.A.H. 1989. Nuclear Magnetic Resonance at microwave frequencies, *Hyperfine Interactions* **51**: 1139.
- CARBONI, C., BUNBURY, D.ST.P. and McCAUSLAND, M.A.H. 2009. Crystal-field anisotropy of TmFe_2 . *To be published*.
- DE AZEVEDO, W.M., MACKENZIE, I.S. and BERTHIER, Y.J. 1985. NMR of $^{159}\text{TbFe}_2$ and TbFe_3 . *J Phys F. Met. Phys.* **15**: L243.
- DE AZEVEDO, W.M. 1986. The hyperfine interaction of terbium in magnetically ordered compounds, PhD thesis, University of Manchester, UK.
- DUMESNIL, K., DUFOUR, C., MANGIN, PH. and ROGALEV, A. 2002. Magnetic springs in exchange coupled $\text{DyFe}_2\text{-YFe}_2$ superlattices: an element selective X-ray magnetic circular dichroism study, *Phys. Rev. B*, **65**: 094401-094406.
- DE LA FUENTE., C., ARNAUDAS, J.I., CIRIA, M., DEL MORAL, A., DUFOUR, C., MOUGIN, A. and DUMESNIL, K. 2001. Magnetic and magnetoelastic behavior of epitaxial $\text{TbFe}_2\text{-YFe}_2$ bilayers, *Phys. Rev. B* **63**: 054417-054427.
- FUJIWARA, A., ASAKURA, K., HARADA, I., OGASAWARA, H. and KOTANI, A. 2005. XMCD study on electronic and magnetic states of rare earth 5d electrons in Laves compounds RFe_2 , *Phys. Scr.* **T115**: 113-114.
- GERMANO, D.J. and BUTERA, R.A. 1981. Heat capacity of, and crystal-field effect in, the RFe_2 intermetallic compounds, *Phys. Rev. B*, **24(7)**: 3912-3927
- GORDEEV, S.N., BEAUJOUR, J-M L., BOWDEN, G.J., RAINFORD, B.D., DE GROOT, P.A.J., WARD, R.C.C., WELLS, M.R. and JANSEN, A.G.M. 2001. Giant magnetoresistance by exchange springs in $\text{DyFe}_2\text{-YFe}_2$ superlattices, *Phys. Rev. Lett.* **87**: 186808-186812.

- GRATZ, E., KOTTAR, A., LINDBAUM, A., MANTLER, M., LATROCHE, M., PAUL-BONCOUR, V., ACET, M., BARNER, C., HOLZAPFEL, W.B., PACHECO, V. and YVON, K. 1996. Temperature and pressure-induced structural transitions in rare-earth deficient RNi₂ Laves phases, *J. Phys.: Condens. Matter* **8**: 8351-8361.
- LEA, K.R., LEASK, J.M. and WOLF, W.P. 1962. The raising of angular momentum degeneracy of *f*-electron terms by cubic crystal field, *Journal of the Physics and Chemistry of Solids*, **23**: 1381-1405.
- LEE, S.J., LANGE, R.J., CANFIELD, P.C., HARMON, B.N. and LYNCH, D.W. 2000. Optical and magneto-optical properties of RFe₂ and RCo₂, *Phys. Rev. B*, **61**: 9669-9679.
- LI Y, CARBONI, C., ROSS, J.W., MCCAUSLAND, M.A.H. and BUNBURY, D.ST.P, 1996. Hyperfine fields at lanthanides nuclei in the intermetallic compounds RFe₂, *J Phys Condens. Matter* **8**: 865.
- MCMORROW, D.F., MCCAUSLAND, M.A.H. and HAN, Z.P. 1989. Exchange and crystal field interaction of Ho³⁺ in GdAl₂ : a single crystal NMR study, *J Phys Condens. Matter* **1**: 10439-10458.
- MCCAUSLAND, M.A.H. and MACKENZIE, I.S. 1979. Nuclear Magnetic resonance in Rare Earth metals, *Adv. Phys.* **28**: 305.
- MOUGIN, A., DUFOUR, C., DUMESNIL, K. and MANGIN, P. 2000. Strain induced magnetic anisotropy in single crystal RFe₂ (110) thin films, *Phys. Rev. B*, **62**: 9517-9531.
- OSTER, J., WIEHL, L., ADRIAN, H. and HUTH, M. 2005. Magnetic and magnetoelastic properties of epitaxial (211)-oriented RFe₂ thin films *J. Mag. Mag. Mater.*, **292**: 164-177.
- PARLEBAS, J.C., ASAKURA, K., FUJIWARA, A., HARAD, I. and KOTANI, A. 2006. X-ray magnetic circular dichroism at rare-earth L23 absorption edges in various compounds and alloys, *Physics Reports*, **431-1**: 1-38.
- PAUL-BONCOUR, V. 2004. Comparison of the influence of hydrogen on the magnetic properties of RMn₂ and RFe₂ Laves phase compounds, *Journal of Alloys and Compounds*, **367**: 185-190.
- SAWICKKI, M., BOWDEN, G.J., DE GROOT, P.A.J., RAINFORD, B.D., BEAUJOUR, J-M L., WARD, R.C.C. and WELLS, M.R. 2000. Exchange springs in antiferromagnetically coupled DyFe₃-YFe₂ superlattices, *Phys Rev B* **62**: 5817-5820.
- STEVENS, K.W.H. 1952. Matrix Elements and Operator Equivalents Connected with the Magnetic Properties of Rare-Earth Ions, *Proc. Phys. Soc. A* **65**: 209-215.
-

Received 24 November 2008

Accepted 23 August 2009